Magnetic Properties of Magnetite Nanoparticles Synthesized by Oxidative Alkaline Hydrolysis of Iron Powder

Nucharee Chomchoey[1,2], Darunee Bhongsuwan[2] and Tripob Bhongsuwan[1]*

ABSTRACT

The black magnetic nanoparticles (MNPs) of magnetite (Fe_3O_4) were synthesized by oxidative alkaline hydrolysis of the atomized iron powder precursor. The synthesized particles prepared at different precipitation temperatures were characterized using X-ray powder diffraction (XRD), the Brunauer–Emmett–Teller (BET) method and transmission electron microscopy (TEM). Their magnetic properties were examined using a vibrating sample magnetometer (VSM), measurement of the initial magnetic susceptibility, acquisition of the isothermal remanent magnetization (IRM) and alternating field (AF) demagnetization of the acquired IRM. The results showed that the sizes of MNPs depended upon the precipitation temperature, which affected the magnetic susceptibility, magnetic hysteresis properties and remanent properties of the synthesized MNPs. The maximum grain size, magnetic susceptibility and magnetic hysteresis properties were obtained from the MNPs synthesized at a precipitation temperature of 70°C. The MNPs prepared by this method exhibited a cubo-octahedral structure with average particle sizes of 25-70 nm. Room temperature magnetic hysteresis properties confirmed the ferromagnetic behavior of stable single domain particles with saturation magnetization of 11.64-77.45 emu/g, remanent magnetization of 1.28-15.769 emu/g, and coercivity of 112.42-158.03 G.

Keywords: cubo-octahedral, magnetite, remanent magnetization, hysteresis properties, single domain

INTRODUCTION

Magnetic nanoparticles (MNPs) have attracted much interest in their applications in various fields, not only in the field of medical care, such as in drug delivery, magnetic hyperthermia and magnetic resonance imaging (Gupta *et al.*, 2004; Yu *et al.*, 2008; Kallumadil *et al.*, 2009), but also in environmental protection (Oliveira *et al.*, 2002; Wu *et al.*, 2005). MNPs have been used widely as a magnetic recording material.

For such practical uses of MNPs, the particle sizes, magnetic properties, and surface properties of the nanoparticles are of great importance. These properties are reported to be influenced by the method of synthesis employed. MNPs have been prepared by various methods. Most studies focused on the preparation of very small nano-sized iron oxide particles with superparamagnetic (SPM) properties. In general, nanoparticles of iron oxides such as Fe_3O_4 and γ-Fe_2O_3 with a diameter in the range of 2 to 20 nm

[1] Department of Physics, Faculty of Science, Prince of Songkla University, Songkhla 90112, Thailand.

[2] Department of Material Science and Technology, Faculty of Science, Prince of Songkla University, Songkhla 90112, Thailand.

* Corresponding author, e-mail: tripop.b@psu.ac.th

are prepared by the common co-precipitation of ferrous and ferric ions at the ratio of 1:2 in an alkaline medium (Sun *et al.*, 2004; Dutz *et al.*, 2007; Mürbe *et al.*, 2008; Chomchoey *et al.*, 2009). Recently, a sol-gel method has been developed for preparation of MNPs, because of their good homogeneity and high purity (Chomchoey *et al.*, 2009). However, phase transformation in the sol-gel method requires a vacuum oven that is not available in many laboratories and makes the method complicated and expensive for MNP production.

The current research involved a detailed investigation of the synthesis of Fe_3O_4 nanoparticles by oxidative alkaline hydrolysis of the iron powder, and characterization and determination of the magnetic properties of Fe_3O_4 particles of single domain size ranges that are favorable for environmental applications because of their high stability.

MATERIALS AND METHODS

Preparation of ferrous precursor

An analytical reagent (12M HCl; 100 ml) was added into 20 g of iron powder AHC 100.29 contained in a 600-mL beaker. The mixture was heated on a hot plate until it turned into a turbid solution, which was heated further until it had dried. The muddy solid obtained was called the ferrous precursor and then used as the starting material to synthesize the MNPs.

Preparation of the MNPs

The MNPs were prepared by dissolving the ferrous precursor (10 g) in 300 mL distilled water. This clear starting solution was heated and maintained at a temperature of 25°C until the end of process. Some 0.5 mol NaOH and oxidizing agent were dissolved in 100 mL distilled water and the mixed solution was added drop-wise into the previous solution at a rate of 2.5 mL min^{-1} and stirring was continued at 350 rpm until the pH of

the solution was raised to 13. The color of solution turned to black indicating that a precipitate of the MNPs had formed. The precipitates were filtered, rinsed with 500 mL distilled water, collected and then air-dried in an oven at 80°C for 3 h. Similar processes were performed at various starting solution temperatures of 50, 70 and 90°C, respectively.

Characterization

The crystallographic structure of the as-synthesized MNPs was characterized by high resolution powder X-ray diffraction (XRD, D/Max-RA, Rigaku, Japan) analysis. The crystallite size was calculated from the XRD pattern using the Scherrer equation (Sun *et al.*, 2004) in Equation 1:

$$d_{XRD} = \frac{K\lambda}{B\cos\theta} \tag{1}$$

The equation uses the reference peak width at angle θ, where λ is the X-ray wavelength (1.54059 Å), B is the width of the XRD peak at half height and K is a shape factor, about 0.90 for magnetite and maghemite.

The specific surface area of the powders was determined by the Brunauer–Emmett–Teller method (BET) (Coulter SA3100, USA). A mean particle size was estimated using Equation 2:

$$d_{BET} = \frac{6}{\rho As} \tag{2}$$

Where ρ is the density and As is the specific surface area of the powders (Dutz *et al.*, 2007; Mürbe *et al.*, 2008).

The surface morphology and grain size of the powders was observed by transmission electron microscopy (TEM, JEOL 2010, 200 kV, Japan).

Several magnetic properties of the synthesized MNPs were examined. The magnetic susceptibility of the MNPs was measured using a spinning Kappabridge (KLY-3S, AGICO, Czech

Republic) and the magnetic hysteresis properties were measured at room temperature using a vibrating sample magnetometer (VSM, Lakeshore 7400) with the inducing field sweeping from -10 to 10 kG. The isothermal remanent magnetization (IRM) was progressively stepwise induced with a strong magnetic field of 0-1 Tesla and was measured at each inducing step using a spinner magnetometer (JR-6, AGICO, Czech Republic). The IRM acquisition curve of the MNPs can be useful to distinguish among: 1) superparamagnetic (SPM), single-domain (SD) or multi-domain (MD) magnetic grains; and 2) the low and high coercivity magnetic components. For example, the IRM of a low coercivity magnetite (Fe_3O_4) reaches saturation at a low inducing field of 30 mT, whereas the IRM of a high coercivity hematite (α-Fe_2O_3) and goethite (α–FeOOH) does not saturate even at a high field of 1 T. The alternating field (AF) demagnetization tests of IRM of the MNP samples were performed using an AF demagnetiser (Molspin, AC Shielded demagnetizer, UK). The AF demagnetization curve can be used to distinguish a high coercivity

phase (i.e. hematite, goethite) that can be co-precipitated from the low coercivity magnetite nano-particles, if the preparation conditions are not appropriate.

RESULTS AND DISCUSSION

Phase study and morphology

The X-ray diffraction patterns of all the samples synthesized at different precipitation temperatures are shown in Figure 1. All diffraction peaks of particles synthesized at temperatures of 70 and 90°C were indexed in the cubic spinel structure (space group Fd3m, 227) for magnetite (Fe_3O_4) (PDF no. 19-0629) and no additional reflections were observed. The samples synthesized at temperatures of 25 and 50°C were indexed in the cubic spinel structure for magnetite (Fe_3O_4), mixed with the orthorhombic structure for goethite (α-FeOOH) (PDF no. 29-0713). However, it was noted that the goethite peaks disappeared at higher precipitation temperatures.

The reaction to produce MNPs was an alkalization reaction of ferrous ions. The following
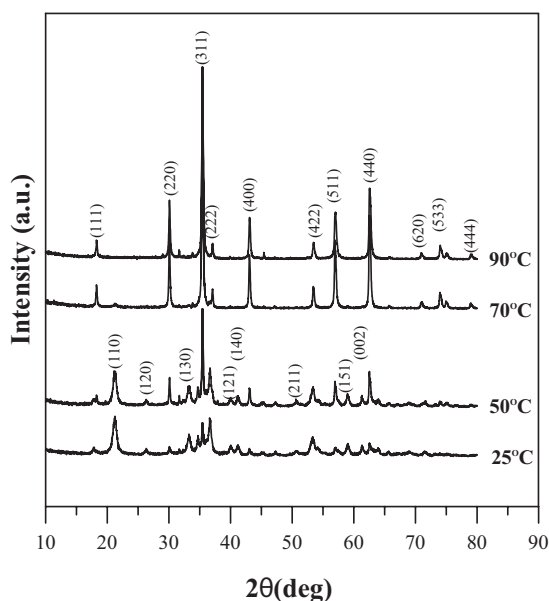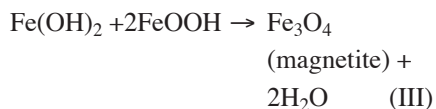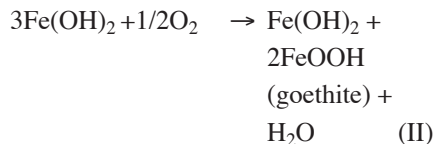

Figure 1 XRD patterns of MNPs precipitated at 25, 50, 70 and 90°C.

reactions for the mechanism of the formation of magnetite (Fe_3O_4) were proposed.

$$Fe^{2+} + 2OH^- \rightarrow Fe(OH)_2 \quad (I)$$
$$3Fe(OH)_2 + 1/2 O_2 \rightarrow Fe(OH)_2 + 2FeOOH \text{ (goethite)} + H_2O \quad (II)$$
$$Fe(OH)_2 + 2FeOOH \rightarrow Fe_3O_4 \text{ (magnetite)} + 2H_2O \quad (III)$$

Therefore, in the synthesis of Fe_3O_4 with ferrous ions alone, as in this case, Fe_3O_4 is formed as a result of the dehydration reaction of ferrous hydroxide and ferric oxyhydroxide (goethite, reaction III), in which the latter compound is produced by the partial oxidation of ferrous hydroxide by O_2 dissolved in the solution (reaction II). This mechanism controls the transformation of the iron hydroxide phases to the final phase of magnetite. The alkalization reactions of the ferrous ions have been extensively studied by Olowe and Refait (Olowe *et al.*, 1991; Refait *et al.*, 1993).

The morphological properties of the synthesized MNPs at different preparation conditions are compared in Table 1. The crystallite sizes (d_{XRD}) as calculated with Scherrer's equation (30-40 nm) were not in agreement with those determined by the BET method (d_{BET}), because at larger crystallite sizes of multi-layer crystals, the d_{XRD} is inaccurate and differs from d_{BET} with a larger degree of uncertainty. The TEM micrographs of the synthesized MNPs precipitated at 70°C showed a clear cubo-octahedral morphology (Figure 2). At this precipitation temperature, the average size of the MNPs

Table 1 Physical properties and magnetic hysteresis properties of the MNPs synthesized at different precipitation temperatures.

Precip. Temp.	As (m^2g^{-1})	d_{BET} (nm)	d_{XRD} (nm)	k (μSI)	Ms (emu/g)	Mr (emu/g)	Hc (G)	Mr/Ms
25°C	47.862	25.07	39±1	10159±65	11.640	1.2830	112.42	0.1102
50°C	33.796	35.51	36±3	19412±32	26.145	3.7258	127.83	0.1425
70°C	17.510	68.53	33±2	52891±1469	77.450	15.769	158.03	0.2036
90°C	18.475	64.95	31±1	43726±799	70.843	13.123	144.93	0.1852

Note: As = specific surface area; d_{BET} = particle size; d_{XRD} = XRD crystallite size; k = magnetic susceptibility; Ms = saturation magnetization; Mr = remanent magnetization; and Hc = magnetic coercivity.
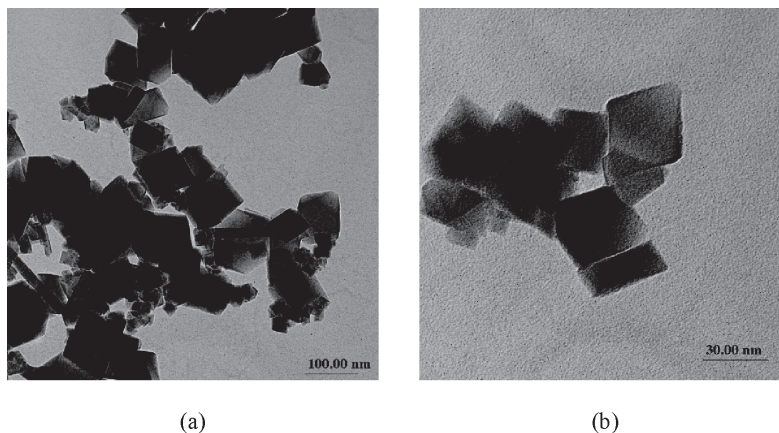

(a)   (b)

Figure 2 TEM micrographs of the synthesized MNPs precipitated at 70°C; (a) at x25,000; and (b) at x100,000 magnification.
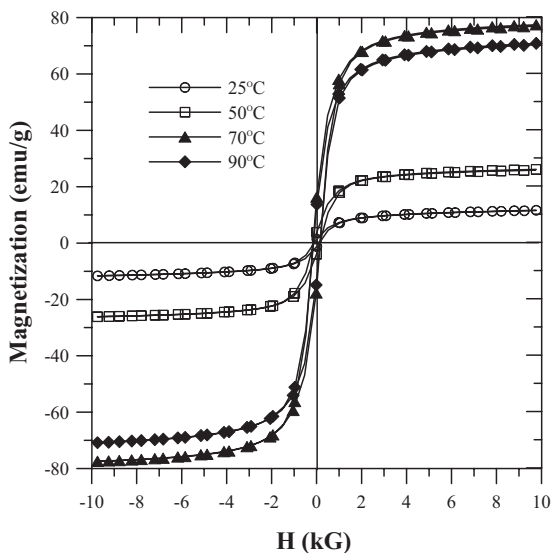
Figure 3 Magnetic hysteresis loop of the synthesized MNPs precipitated at temperatures of 25, 50, 70 and 90°C.

measured from the TEM image was about 60-70 nm, which was in agreement with those determined from the BET technique.

Magnetic properties

The M–H relation or magnetic hysteresis loops (Figure 3) of the MNPs prepared at different precipitation temperatures show typical ferromagnetic behavior with a trace of a high coercivity phase that is interpreted as goethite (see reaction III). The saturation magnetization (Ms) of the MNPs increased when the precipitation temperature increased and reached the maximum Ms (77.45 emu/g) for the MNPs precipitated at 70°C. At a precipitation temperature of 90°C, the Ms of the MNPs decreased to 70.843 emu/g. This probably implies the effect of chemical concentrations and a precipitation temperature that inhibited the formation of magnetite (reaction III), resulting in a reduction in the grain size of the MNPs (Figure 4a) and a reduction in the total magnetization of the MNPs (Figure 4c). It can be concluded that the sizes of synthesized magnetite MNPs depend on the precipitation temperature and

can be estimated from their values for k, Ms and Mr (Figure 4).

The magnetic hysteresis studies of the MNPs synthesized at 70°C in the present method and synthesized by two other methods, namely, the co-precipitation method (Chomchoey *et al*., 2009) and the sol-gel method (Chomchoey *et al*., 2009), are compared in Figure 5. The coercivity (Hc) and the saturation magnetization (Ms) of the MNPs increased with increasing particle size (reported in Table 2 by Hc = 34.0, 21.1, and 158.03 G and Ms = 63.2, 52.2, and 77.450 emu/g for the samples with d_{BET} 11.48, 11.26 and 68.53 nm, respectively).

The ratio Mr:Ms and the Hc of the MNPs prepared by the co-precipitation and sol-gel methods were very low, indicating a large proportion of superparamagnetic (SPM) grains consistent with an average grain diameter of 11 nm by the BET method. The ratio Mr:Ms (0.2) and the Hc (158 Oe) of the MNPs prepared using the present method (in the current study) at a precipitation temperature of 70°C were high, indicating that they possessed the magnetic
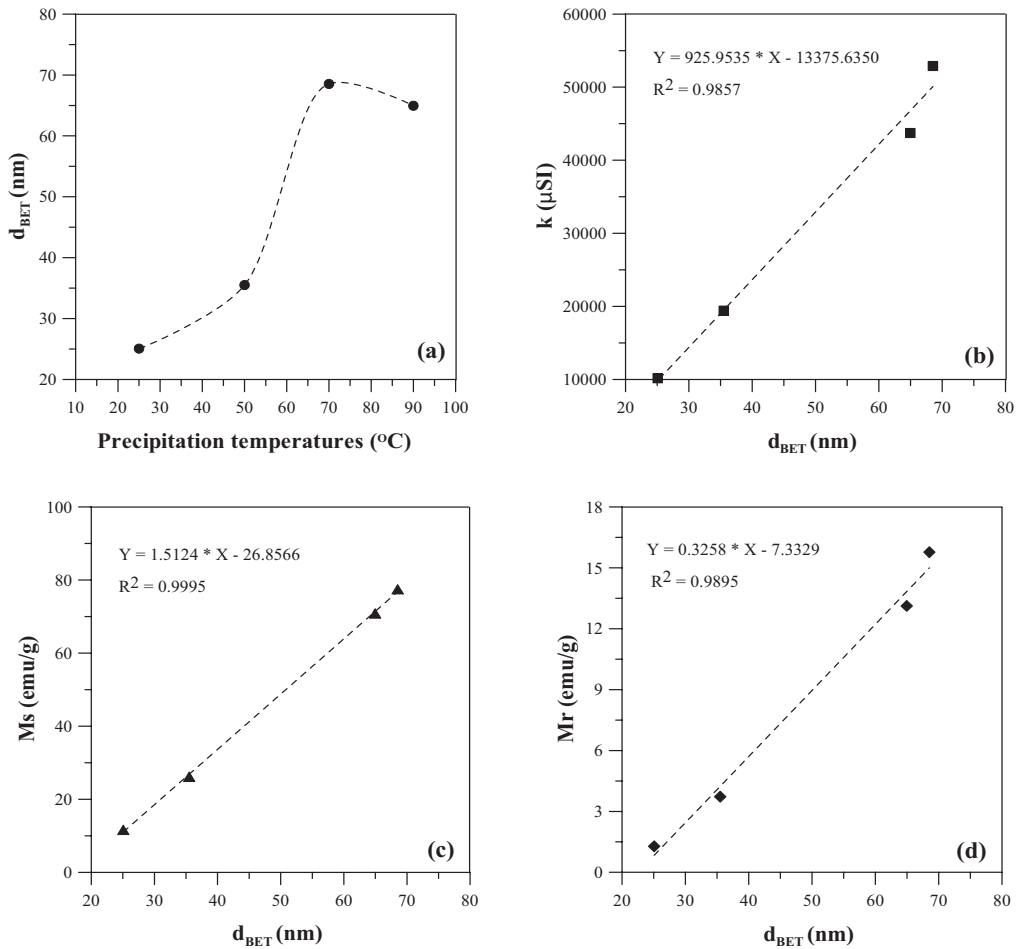
Figure 4 Relationship between the physical properties and magnetic properties of the MNPs; (a) d_{BET} versus precipitation temperature; (b) k versus d_{BET}; (c) Ms versus d_{BET}; and (d) Mr versus d_{BET}.

Table 2 Comparison of physical and magnetic properties of the MNPs prepared by different methods.

Method	As (m^{2}g^{-1})	d_{BET} (nm)	d_{XRD} (nm)	k (μSI)	Ms (emu/g)	Mr (emu/g)	Hc (G)	Mr/Ms
Co-precipitation	104.49	11.48	12.70	69986±1333	63.2	2.4	34.0	0.0387
Sol-gel	106.50	11.26	12.23	113207±2413	52.2	1.3	21.1	0.0258
Present method	17.51	68.53	31-35	52891±1469	77.450	15.769	158.03	0.2036

Note As=specific surface area; d_{BET}=particle size; d_{XRD}=crystallite size; k=magnetic susceptibility; Ms=saturation magnetization; Mr= remanent magnetization and Hc= coercivity.
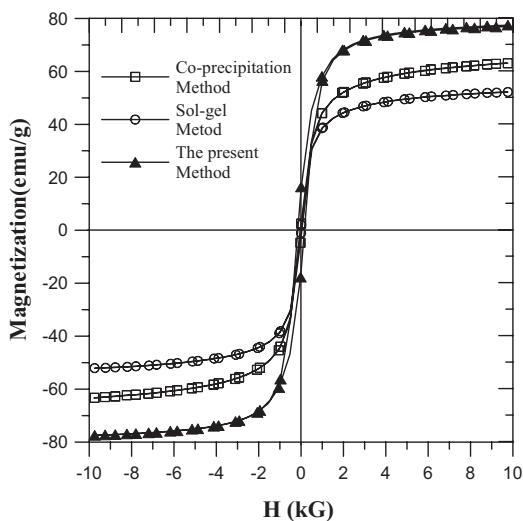
Figure 5 Magnetic hysteresis loop of the MNPs prepared by three different methods.

Figure 6 IRM acquisition curves of the MNPs prepared by three different methods.

properties of single domain (SD) grains. This agreed with the MNPs grain size measured by TEM (60-70 nm) and by the BET technique of 68.5 nm. Several experimental studies have confirmed a critical size of $d_{SPM} < 30$ nm for SPM grains (McNab *et al.*, 1968; Dunlop and Bina, 1977) and single domain cubic magnetite particles have been experimentally observed below 60 nm (Dunlop, 1973), and theoretically below 84 nm (Enkin and Dunlop, 1987; Enkin and Williams, 1994).

Figure 6 shows the IRM acquisition curves for typical MNPs samples prepared by the three different methods. In general, with increasing applied magnetic field, all samples were easily saturated in their IRM at a low inducing field (under 0.3 T). The saturation IRM (SIRM) of samples prepared by the co-precipitation, sol-gel and present methods were 94.881, 50.842 and 940.909 A/m, respectively, indicating the presence of a magnetically soft ferromagnetic phase, interpreted as magnetite. This result was consistent with the results of the AF demagnetization of IRM shown in Figure 7. It was found that an AF field
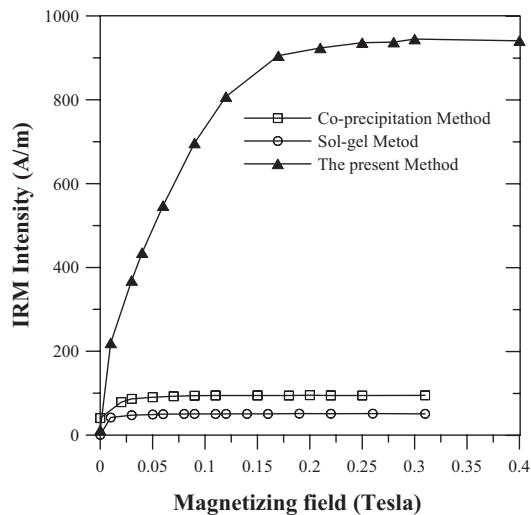
of 30 mT can demagnetize almost totally the SIRM (>95%) of all samples. This indicates no high coercivity magnetic phase (i.e. goethite and hematite) was formed in the synthesized MNPs in all three methods.
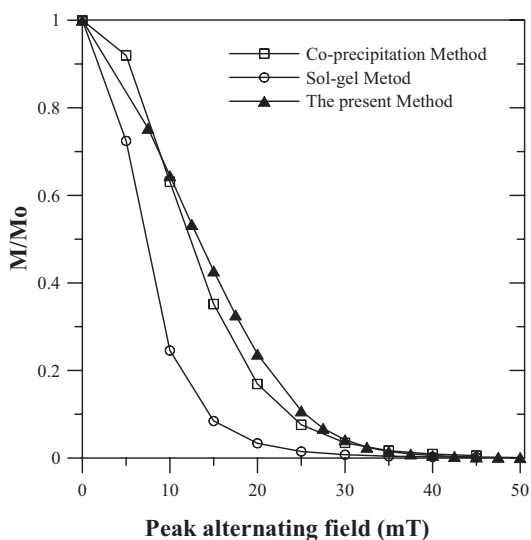

Figure 7 AF demagnetization of IRM of the MNPs prepared from the three methods.

CONCLUSIONS

Magnetite nanoparticles (Fe_3O_4) with cubo-octahedral crystal structures and an average particle size of 25-70 nm were successfully synthesized by oxidative alkaline hydrolysis of atomized iron powder (AHC 100.29). The precipitation temperature was the important factor controlling the particle sizes of the MNPs. The magnetite MNPs sized 68 nm were the biggest prepared by this method at a precipitation temperature of 70°C.

The morphology, magnetic hysteresis properties and remanance properties of the MNPs prepared using the present method indicated that they possess magnetite nanoparticles of single domain grains with a saturation magnetization of 77.450 emu/g, a remanent magnetization of 15.769 emu/g, a coercivity of 158.03 G and a saturation IRM of 940.909 A/m. Moreover, the analysis showed that magnetic hysteresis properties can be used as an alternative tool to estimate the average size of the single domain magnetite grains, because their magnetic properties are observed to be linearly proportional to their particle sizes (d_{BET}) with the R^2 values equal to 0.9857, 0.9995 and 0.9895 for the susceptibility value, saturation magnetization and remanent magnetization, respectively.

ACKNOWLEDGEMENTS

LITERATURE CITED

Chomchoey, N., T. Bhongsuwan and D. Bhongsuwan. 2009. Remanent Magnetization Characteristics of Synthetic Magnetic Nanoparticles. **KKU Research Journal (Graduate Studies)** 9: 48-56.

Dunlop, D.J. 1973. Superparamagnetic and single-domain threshold size in magnetite, **J. geophys. Res.** 78: 1780-1793.

Dunlop, D.J. and M.M. Bina. 1977. The coercive force spectrum of magnetite at high temperature: Evidence for thermal activation below the blocking temperature. **Geophys. J. R. Astron. Soc.** 51: 121-147.

Dutz, S., R. Hergt, J. Mürbe, R. Müller, M. Zeisberger, W. Andrä, J. Töpfer and M.E. Bellemann. 2007. Hysteresis losses of magnetic nanoparticle powders in the single domain size range. **J. Magn. Magn. Mater.** 308: 305-312.

Enkin, R.J. and D.J. Dunlop. 1987. A micromagnetic study of pseudo-single-domain remanence in magnetite. **J. Geophys. Res.** 92: 12726-12740.

Enkin, R.J. and W. Williams. 1994. Three dimensional micromagnetic analysis of stability in fine magnetic grains. **J. Geophys. Res.** 99: 611-618.

Gupta, A.K. and S. Wells. 2004. Surface-modified superparamagnetic nanoparticles for drug delivery: preparation, characterization, and cytotoxicity studies. **IEEE Transac. Nanobioscience.** 3: 66-73.

Kallumadil, M., M. Tada, T. Nakagawa, M. Abe, P. Southern and Q.A. Pankhurst. 2008. Suitability of commercial colloids for magnetic hyperthermia. **J. Magn. Magn. Mater.** 321: 1509-1513.

McNab, T.K., R.A. Fox and A.J.F. Boyle. 1968. Some magnetic properties of magnetite microcrystals. **J. Appl. Phys.** 39: 5703-5711.

Mürbe, J., A. Rechtenbach and J. Töpfer. 2008. Synthesis and physical characterization of magnetite nanoparticles for biomedical applications. **Mater. Chem. Phys.** 110: 426-433.

Oliveira, L.C.A., R.V.R.A. Rios, J.D. Fabris, V. Garg, K. Sapag and R.M. Lago. 2002. Activated carbon/iron oxide magnetic composites for the adsorption of contaminants in water. **Carbon.** 40: 2177-2183.

Olowe, A.A. and J.M.R. Génin. 1991. The mechanism of oxidation of ferrous hydroxide in sulphated aqueous media: Importance of the initial ratio of the reactants. **Corros. Sci.** 32: 965-984.

Powder Diffraction file No. 19-0629, **International Centre for Diffraction Data**, Newton Square, PA, 2002.

Powder Diffraction file No. 29-0713, **International Centre for Diffraction Data**, Newton Square, PA, 2002.

Refait, Ph. and J.M.R. Génin. 1993. The oxidation of ferrous hydroxide in chloride-containing aqueous media and pourbaix diagrams of green rust one. **Corros. Sci.** 34: 797-819.

Sun, Y.K., M. Ma, Y. Zhang and N. Gu. 2004. Synthesis of nanometer-size maghemite particles from magnetite. **Colloids and Surf. A** 245: 15-19.

Wu, R., J. Qu and Y. Chen. 2005. Magnetic powder $MnO-Fe_2O_3$ composite -a novel material for the removal of azo-dye from water. **Wat. Res.** 39: 630-638.

Yu, M.K., Y.Y. Jeong, J. Park, S. Park, J.W. Kim, J.J. Min, K. Kim and S. Jon. 2008. Drug-Loaded Superparamagnetic Iron Oxide Nanoparticles for Combined Cancer Imaging and Therapy In Vivo. **Angew. Chem. Int. Ed.** 47: 5362-5365.